13th World Conference on Earthquake Engineering
Vancouver, B.C., Canada
August 1-6, 2004
Paper No. 2274

A SIMPLE PROCEDURE TO COMPUTE THE INTERSTORY DRIFT FOR FRAME TYPE STRUCTURES

Sinan AKKAR[1], Polat GÜLKAN[1] and Ufuk YAZGAN[1]

SUMMARY

A simple procedure to estimate the local displacement demands in regular frame type structures is described. Given the spectral displacement and beam-to-column stiffness ratio, the procedure calculates the maximum ground story and maximum interstory drifts along the height of the structure. A total of 145 near-fault ground motions recorded on dense-to-firm soil sites are used for the evaluation of the procedure. The approximate drift demands computed from this procedure and the exact results from 27550 response history analyses are used for calculating the error statistics. The calculations show that the procedure can be used with confidence for frames with fundamental periods between 0.3s and 1.5s when they are subjected to near-fault records without pulse. The approximations are in good agreement with the exact response history results of near-fault records with pulse when the fundamental period to pulse period ratio is less than 1.5. The performance of the new procedure is also compared with other approximate methods that are employed for similar purposes.

INTRODUCTION

Recent improvements in earthquake engineering require more quantified descriptions of seismic demand parameters that form an important context within the decision stage of structural design and performance assessment. As a consequence, considerable work has been done to understand the variation of global and local displacement demands along the structural elevations leading to more accurately established displacement levels that must be met at a given seismic hazard level and performance state. One of the corner stones that have stimulated these efforts was the 1994 Northridge earthquake that showed the extent of economical and functionality losses due to the insufficient lateral displacement capacity of framed structures. The high displacement demands submerged in the near-fault ground motion records of the Northridge earthquake were observed a year later in the 1995 Kobe earthquake where a monetary loss of about US$200 billion was reported by EERI [1]. These effects were mostly concentrated in engineered structures. As indicated by Sasani [2], near-fault records with extensive displacement demands are not pertinent to those two earthquakes. However, concerns on these unanticipated structural failures with significant downtime payments have led to extensive research projects to re-examine the relationship between local displacement demand and structural capacity during the last decade (e.g. SAC steel

[1] Department of Civil Engineering, and Disaster Management Research Center, Middle East Technical University 06531 Ankara, Turkey.

project). The studies of Gupta [3], Luco [4] and MacRae [5] that are generated by these projects investigated the variation of seismic drift demands on certain structural types when they are subjected to critical actual or simulated near-fault ground motions with different probability levels. The principal information derived from these investigations has indicated how local displacement demand variation might become complex due to the significant uncertainty in near-fault ground motion as they interact with structural parameters. Researchers like Atalla [6] and Krawinkler [7] noted that the interaction between the structural period and the pulse period of near-fault records that are affected by forward directivity has an important effect on local structural displacements.

Although the determination of local displacement demands due to earthquake induced ground motions have become attractive for the last decade, the ground breaking studies can be traced to the 1930s. Westergard [8] described how structural displacements could become critical under pulse signals. Heidebrecht [9] derived the lateral displacements and associated internal stresses by solving the fourth order partial differential equation that represents the flexural and shear behavior and other systems that fall between these two extremes. Iwan [10] proposed the drift spectrum as a complement to the response spectrum to describe the local displacement demand of pulse-like, near-fault earthquake records. His drift spectrum is based on the solution of damped shear waves propagating along a shear beam, and computes the drift by analogy with the shear strain of a shear beam. Heidebrecht and his co-workers [11, 12] described another method for defining ground story drift using one-dimensional wave propagation along a shear beam and response spectrum concept. Using the fourth order differential equation described by Heidebrecht [9], Miranda [13] derived a maximum interstory drift expression for uniform lateral stiffness general structural behavior (i.e. frames deforming both in shear and flexure). Recently, Miranda [14] has shown that the maximum interstory drift difference between uniform and non-uniform lateral stiffness cases is insignificant in the elastic range. Using the shear beam concept together with response history analysis, Chopra [15] indicated that the drift spectrum proposed by Iwan could be duplicated by using a total of 5 modes for undamped cases. Gülkan [16] defined an alternative expression for drift spectrum and showed that the shear beam fundamental mode and response spectrum concepts could be combined to the ground story drift within an error bound of 10 percent for shear frames with fundamental periods less than 2s under near-fault ground motions. Except for Miranda [13], the work cited above describes the interstory drift demands by analogy of a shear beam model that generally yields the maximum interstory drift at the ground level due to the physical constraints in the model. However, the girder/column stiffness relation plays a role in structural displacement patterns, and shear beam approach may not represent the general moment resisting frame (MRF) behavior.

The objective of this article is to describe a procedure to estimate the maximum ground story and maximum interstory drift for MRF behavior. The proposed procedure is based on modal analysis concept. It modifies the drift expression presented in Gülkan [16] that utilizes the first mode shear beam deformation pattern, combining it with spectral displacement. The improved procedure uses beam-to-column stiffness ratio to account for the general MRF behavior, and modifies the local displacement demands computed by the shear beam behavior. Using a total of 145 near-fault ground motions, the applicability of the new procedure is evaluated for frame structures with fundamental periods between 0.2s to 2.0s. In the ground motion data set, 56 near-fault records contain pulse in their waveforms. In order to achieve a more specific verification of the procedure, the evaluation is conducted separately for ground motions with and without pulse signals. Error statistics are presented to demonstrate how certain near-fault ground motion features seem to influence the performance of the proposed procedure. The accuracy of the procedure is compared with similar expressions derived by Miranda [13] and Iwan [10] for general frame behavior and shear frame behavior, respectively. These results might be useful in the preliminary design stage or during a quick seismic performance assessment of existing structures.

BASIC THEORY

Modal analysis

The modal analysis describes the lateral displacements of a multi-degree-of-freedom (MDOF) system subjected to a ground acceleration $a_g(t)$ by

$$u_i(t) = \phi_i \Gamma_i D_i(t) \tag{1}$$

In this expression, ϕ_i and Γ_i are the mode shape and modal participation factor for the ith mode, respectively. The displacement response history $D_i(t)$ is computed by solving the single-degree-of-freedom (SDOF) system equation:

$$\ddot{D}_i(t) + 2\xi_i \omega_i \dot{D}_i(t) + \omega_i^2 D_i(t) = -a_g(t) \tag{2}$$

In Equation (2), ξ_i and ω_i are the viscous damping and circular frequency of the ith mode, respectively. The maximum response u_{max} for the first mode is then computed by using the spectral displacement value $S_d(T,\xi)$ at the fundamental period T and damping ratio ξ:

$$u_{\max} = \phi_1 \Gamma_1 \left| D_1(t) \right|_{\max} = \phi_1 \Gamma_1 S_d(T,\xi) \tag{3}$$

The above equation indicates that given two systems with the same period and viscous damping, the lateral displacements are directly proportional to the product of $\phi_1\Gamma_1$ as the spectral displacement will be the same for these two systems. In the first mode response, the contribution to the ground story displacement is represented by

$$C_{gr} = \Gamma_1 \phi_1^{gr} \tag{4}$$

Similarly, the contribution of the first mode to the top story displacement is

$$C_{top} = \Gamma_1 \phi_1^{top} \tag{5}$$

In Equations (4) and (5), ϕ_1^{gr} and ϕ_1^{top} are the first mode shape values at the ground and top story, respectively. In this article C_{gr} and C_{top} are designated as ground story and top story displacement contribution factors, respectively.

Effect of beam-to-column stiffness ratio (ρ) on lateral displacement patterns

Blume [17] defined the beam-to-column stiffness ratio, ρ, as a parameter that governs the behavior of frame type building systems. It is the ratio of sum of the beam stiffnesses to column stiffnesses at the story that is closest to the mid-height of the building, and it is constant for structures that have uniform lateral stiffness along their height. With the same modulus of elasticity for girders and columns, the general form of ρ is given by

$$\rho = \frac{\sum_{beams} (I/l)_b}{\sum_{columns} (I/l)_c} \tag{6}$$

The ratios $(I/l)_b$ and $(I/l)_c$ are measures of beam and column rigidities. The frame behavior is governed by flexure as ρ diminishes. The larger values of ρ imply shear behavior. The smaller ρ values indicate that columns are stiffer than the girders.

The variation of ρ has a significant effect on the structural displacement. The curves in Figure 1 show the normalized fundamental mode shapes and corresponding interstory drift for frames with different ρ values. These curves are drawn for dimensionless height. The mode shapes are normalized with respect to the top modal displacement. The modal interstory drifts are normalized with respect to their maximum values. The mode shape for ρ = 0.0 represents "flexural" behavior. As ρ increases, the behavior is controlled by both shear and flexural displacements. When ρ becomes large, the structure acts as a "shear" frame. The normalized mode shapes in Figure 1 indicate that the increase in ρ increases the lateral displacement for the fundamental mode. The largest difference between the lateral displacements occurs when ρ is between 0.0 and 0.125 (transition from flexural to combined mode behavior). The lateral displacement changes more gradually when ρ is greater than 0.125. The interstory drift for the first mode behavior also changes significantly for ρ between 0.0 and 0.125. The maximum interstory drift shifts from the upper half of the frame to lower half for ρ between 0.0 and 0.125. The shift of maximum interstory drift to lower stories is very rapid for $0.0 < \rho < 0.125$. In extreme cases, when the structure behaves as a flexural cantilever ($\rho = 0.0$) or in pure shear ($\rho = \infty$), the maximum interstory drift occurs at the top or at the ground story, respectively, if the structural behavior is represented by the first mode. The comparison of the fundamental mode lateral displacements and interstory drift curves for $\rho \geq 0.125$ indicate that the MRF interstory drift variation is more sensitive to the changes in ρ with respect to lateral displacements. For a particular ρ, the relative insensitivity of mode shapes to the bay number supports this observation either for single- or multi-bay frames.

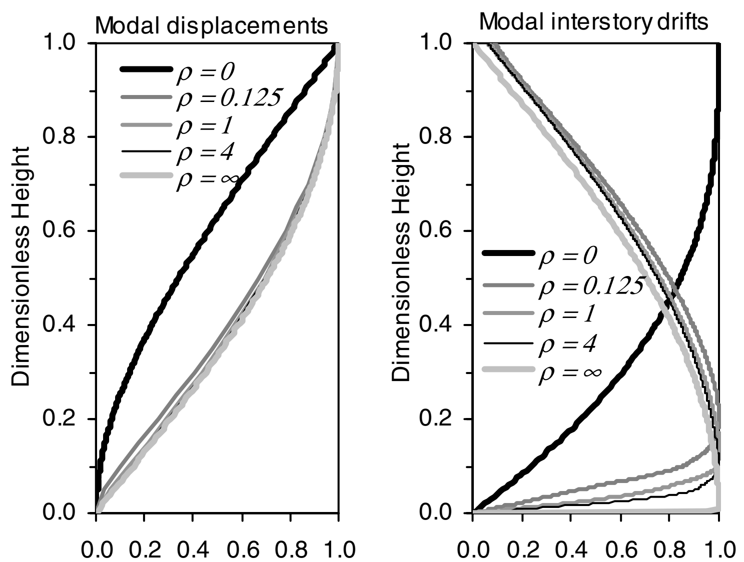

Figure 1. Dependence of lateral deformation on *ρ* for first mode

The period-dependent variation of normalized first mode ground story ($C_{gr}^{\rho=\rho i}$) and top story ($C_{top}^{\rho=\rho i}$) displacement contributions by the corresponding shear frame contributions (i.e. $C_{gr}^{\rho=\infty}$ or $C_{top}^{\rho=\infty}$) are shown in Figures2.a and 2.b, respectively. The curves are drawn for various ρ values. The normalization gives a more descriptive view for the effect of shear frame behavior on the general frame displacements. The curves in Figure 2.a show a strong dependence of ground story drift on beam-to-column stiffness ratio. As the structure shifts from shear frame behavior to combined mode behavior governed by both shear and flexure, the ground story displacement becomes smaller (i.e. $C_{gr}^{\rho=\rho i} / C_{gr}^{\rho=\infty} < 1$). The top story displacement is less sensitive to the changes in *ρ* as it is affected to a lesser extent by variations in ρ. The curves in Figure 2.b show that the top story displacement tends to increase with respect to shear frame for very small ρ values ($\rho \leq 0.01$) when flexural behavior is very dominant. The highlighted observations suggest that the shear frame behavior can accurately estimate the top story displacement for frames with $\rho > 0.01$. This is not the case for ground story drift and estimations based on shear frame behavior would probably overestimate the local ground motion demands as the associated ground story displacements become smaller for decreasing ρ.

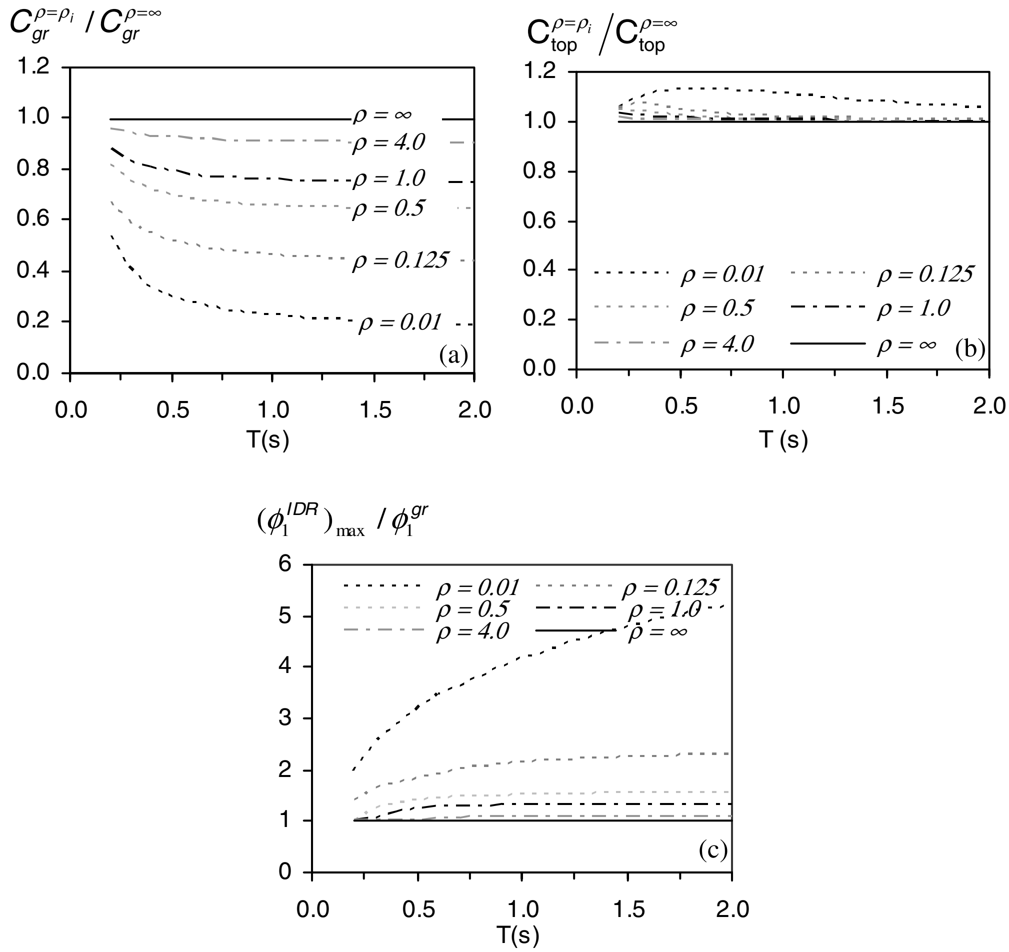

Figure 2. Period dependent variation of ground story and top story displacements with respect to shear frame for different ρ (Figures 2.a and 2.b). Figure 2.c displays the period dependent amplification of maximum interstory drift with respect to ground story drift for different ρ

The discussion on Figure 1 indicated how maximum interstory drift locations change along the elevation for different beam-to-column stiffness ratios. The variation of maximum interstory drift is described in Figure 2.c by plotting the ratio of first mode maximum modal interstory drift $(\phi_1^{IDR})_{max}$ to modal ground story drift (ϕ_1^{gr}). Similar to Figures 2.a and 2.b, the plots are in terms of fundamental period and different ρ values. The ratios show the change in maximum interstory drift with respect to ground story drift for a given ρ value. The amplification of maximum interstory drift relative to ground story drift increases greatly for decreasing ρ values. The increase is more stable as the fundamental period becomes larger. Inherent from the theoretical first mode behavior, the maximum interstory drift always occurs at ground story level for shear frames ($\rho = \infty$).

ESTIMATION OF MAXIMUM GROUND STORY AND MAXIMUM INTERSTORY DRIFT FOR MOMENT RESISTING FRAMES

The maximum ground story drift ratio of shear frames ($GSDR_{sh}$) can be approximated by using Equation (3). Using the first mode shape of a uniform, continuous shear beam and inserting the corresponding modal participation factor will yield the equation proposed by Gülkan [16].

$$GSDR_{sh} = 1.27\, sin\left(\frac{\pi h}{2H}\right)\frac{S_d(T,\xi)}{h} \tag{7}$$

The terms H and h in Equation (7) represent the frame height and story height, respectively. Using the empirical relationships between the building fundamental period and building height (i.e. $T=aH^b$ for generality), Equation (7) can be expressed in an alternative way as presented by Gülkan [16]

$$GSDR_{sh} = 1.27\, sin\frac{\pi\sqrt[b]{a}\,h}{2\sqrt[b]{T}}\frac{S_d(T,\xi)}{h} \tag{8}$$

Either of Equations (7) or (8) can form the basis for estimating the maximum ground story drift (GSDR) and maximum interstory drift (MIDR) ratios. The smooth variation of first mode ground story displacement contribution with respect to shear frame contribution is used to modify Equations (7) and (8) to compute ρ dependent GSDR. Fitting smooth curves to the ratio $C_{gr}^{\rho=\rho i}$ / $C_{gr}^{\rho=\infty}$ presented in Figure 2.a gives the modification factor as a function of fundamental mode period T and ρ. The curve fitting is done by regression analysis that is based on minimizing the square root of the differences (error) between the exact variation and the curve fits. The expressions for the modifying factor are given in Equation (9).

$$\gamma_1(\rho,T) = a(\rho) + \frac{b(\rho)}{T}; \qquad a(\rho) = \frac{1}{1+0.35/\rho^{0.65}}, \quad b(\rho) = \frac{1}{8+25\rho^{0.4}} \tag{9}$$

The term γ_1 is the modification factor that corrects the shear frame ground story drift to a more general, ρ based ground story drift demand expression:

$$GSDR(T,\xi,\rho) = \gamma_1(\rho,T)GSDR_{sh}(T,\xi) \tag{10}$$

Note that the function γ_1 becomes 1 as ρ tends to large values, satisfying the limiting condition for shear frame behavior.

The maximum interstory drift for MRF behavior can be estimated through Equation (10) and the curves presented in Figure 2.c for the first mode variation of maximum interstory drift with respect to the ground story drift. As in the case of Equation (9), the regression analysis was conducted to fit curves on the plots of Figure 2.c to represent the second modification factor γ_2 that accounts for the variation of maximum interstory drift with respect to ground story drift. The function γ_2 should be taken as 1 whenever it gives values less than 1 for a particular T and ρ. The results of the regression analysis are summarized in Equation (11).

$$\gamma_2(\rho,T) = e^{\left(c(\rho)-\frac{d(\rho)}{T}\right)}; \qquad c(\rho) = \frac{1}{2\rho+1}, \qquad d(\rho) = \frac{0.07}{\rho^{0.25}} \tag{11}$$

The modifying factor γ_2 is equal to 1 for large ρ. This satisfies the theoretical limiting conditions between the maximum interstory drift and ground story drift for shear frames. The expression of maximum interstory drift for general MRF behavior is given in Equation (12).

$$MIDR(T,\xi,\rho) = \gamma_1(\rho,T)\gamma_2(\rho,T)GSDR_{sh}(T,\xi) \tag{12}$$

The expressions in Equations (10) and (12) represent the variation of GSDR and MIDR for $\rho \geq 0.125$ that is the practical range of concern in most frame type structures. They are based on theoretical modal analysis concept that is independent of the ground motion. The ground motion characteristics are inherently accounted for by the S_d term that is presented in the base expressions Equations (7) and (8). The elastic local displacement demand estimations of Equations (10) and (11) can be extended to nonlinear range via expressions that relate the elastic and inelastic building displacements through different yield mechanisms (e.g. Seneviretna [18]). However, the warranty is limited for such a modification in the proposed method as the main focus of the study is confined to the detailed evaluation of local displacement estimations from Equations (10) and (12).

EVALUATION OF THE PROPOSED PROCEDURE

A total of 145 near-fault ground motions with moment magnitudes M_w between 6.0 and 7.6 were used in the evaluation of the equations proposed for estimating the GSDR and MIDR. The near-fault ground motions are records from soil site classes that have shear wave velocities between 180 m/s and 760 m/s in the upper 30 m. The closest site-to-fault distances (d) of these records vary from 0.1 km to 20 km. The ground motion data set was divided into two groups as records with and without pulse signals. The velocity waveforms were chosen to identify the pulse signals, as it is easier to detect the pulse from the velocity. The illustrative examples for velocity traces with and without pulse are shown in Figure 3. A total of 56 near-fault records contain pulse signals in the chosen data set. The remaining records do not exhibit a dominant pulse in their waveforms. The complex seismological aspects of near-fault records do not fall within the scope of this text and no further discussion is made on the source and wave propagation effects for pulse dominant near-fault records. The reader is referred to Akkar [19] for a detailed description of the ground motion features used in this study. The pulse periods (T_p) that are computed from the velocity traces of NF records with pulse are compared with the spectral period (T_{pv}) that corresponds to the peak amplitude of the pseudo velocity spectrum (PSV). The correlation between T_p and T_{pv} is given in Figure 4. The strong correlation indicates the dependence of spectral quantities on the pulse signal waveforms. The proposed expressions for MIDR and GSDR would be expected to be sensitive to the demand due to pulse as the spectral displacement term in Equations (10) and (12) is directly related to pseudo-velocity. Therefore, the local displacement demand estimates of the proposed procedure would be reasonable, as long as the first mode behavior governs.

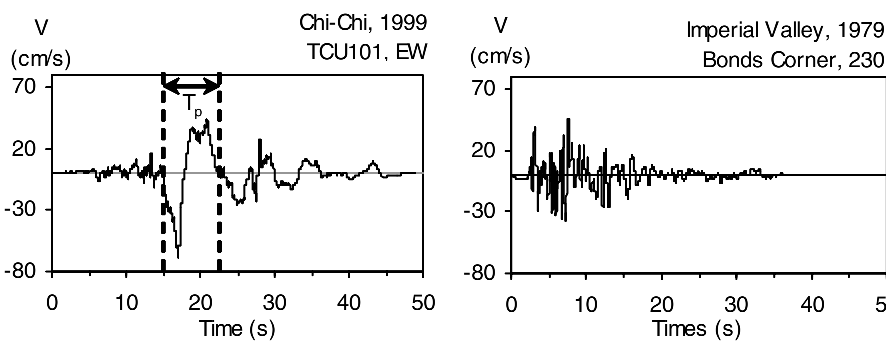

Figure 3. Velocity time series with and without pulse signals

Response history analyses using these records were conducted for a group of 5 percent damped, single bay frame models. A total of 19 generic frame models were used with fundamental mode periods ranging from 0.2s to 2.0s. The fundamental periods of the models change at an interval of 0.1s and in the interest of uniformity they were adjusted to satisfy $T = 0.1n$ where n designates the total number of stories. The story height, h, was taken as 3m for the models. The beam-to-column stiffness ratio (ρ) for the models were varied as ρ = 0.125, 0.25, 0.5, 0.75, 1.0, 1.5, 2.0, 3.0, 4.0, ∞. In this way, the evaluation of the proposed procedure was established by a total number of 190 (19×10) frame models. The number of response history analyses conducted for the evaluation stage was 27550 (19×10×145).

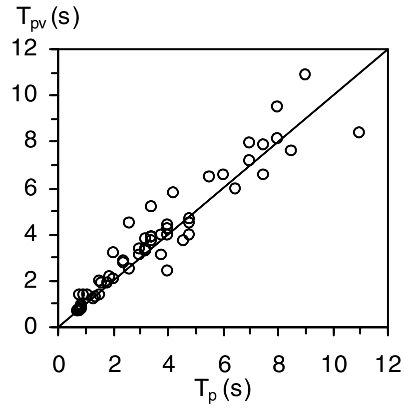

Figure 4. Correlation between T_p and T_{pv}

Effect of near-fault ground motions on MDOF system response

The maximum interstory drift scatter for the near-fault records with and without pulse signals is plotted in Figure 5. For near-fault records with pulse, at each response history run, the fundamental period of the model was normalized with respect to the pulse period of the excitation in order to bring forward the pulse signal effect on the local displacement demand parameter MIDR. The corresponding scatter data shows enhanced amplification when the fundamental periods of the frame systems match the pulse signal period (i.e. $T/T_p \approx 1$). As the fundamental period moves away from the pulse period of the records, the amplifications in the maximum interstory drift ratio tend to fall down. The scatter plots of near-fault records without pulse do not show a clear trend for this case indicating that the MIDR values vary randomly from record-to-record. The scatter plots of GSDR are not shown in this article but they exhibit a similar trend for near-fault records with and without pulse as in the case of MIDR.

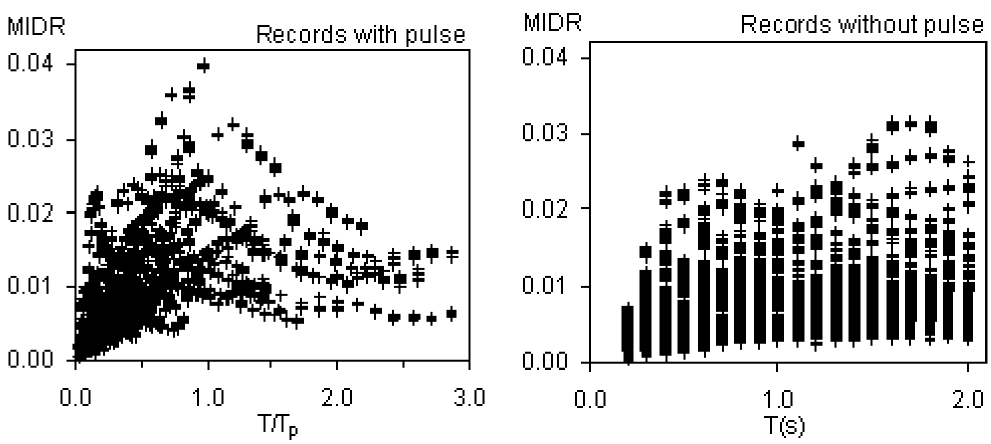

Figure 5. Scatter diagrams for MIDR computed from response history analyses when frame models were subjected to records with and without pulse

Statistical verification - fundamental mode response in capturing the local displacement demand

The estimates of *GSDR* and *MIDR* were evaluated by defining the following error term

$$E = \frac{\Delta_{app}}{\Delta_{exact}} \tag{13}$$

In Equation (13), Δ_{app} designates either the approximate maximum ground story or interstory drift ratios computed from Equations (10) or (12), respectively. The variable Δ_{exact} is the corresponding value resulting from response history analysis when all modes are considered. Given a ground motion record, k, the error term $(E_{T,\rho})_k$ is computed for the fundamental period T and beam-to-column stiffness ratio ρ. The corresponding mean error is calculated by

$$\overline{E}_{T,\rho} = \frac{1}{n_k}\sum_{k=1}^{n_k}\left(E_{T,\rho}\right)_k \tag{14}$$

In Equation (14), n_k is the number of ground motions used in the statistical verification. In this study, it is 56 for pulse dominant near-fault records and 89 for near-fault record data set of no pulse. A mean error value smaller than 1 will indicate that on average, the approximation yields values less than the exact value computed from the response history analyses. A mean error that is larger than 1 will show that on average, the estimates are on the conservative side. The dispersion on the mean estimates is measured by computing the standard deviation of the error given in Equation (15).

$$\sigma_{T,\rho} = \sqrt{\frac{1}{n_k}\sum_{k=1}^{n_k}\left[(E_{T,\rho})_k - (\overline{E}_{T,\rho})_k\right]^2} \tag{15}$$

The mean error trends in GSDR and MIDR estimations for pulse signal near-fault data set are shown in Figure 6 when ρ ranges from 0.125 to ∞. The curves are presented in the non-dimensional period format (i.e. fundamental periods normalized with respect to the period of the pulse in the ground motion). On average the approximate method estimations yield an error of ±10 percent for GSDR and MIDR when $T/T_p \leq 1.5$. As beam-to-column stiffness ratios increase, the mean estimates tend towards the unsafe side. For $T//T_p > 2.2$, the unsafe errors in MIDR grow rapidly and reach 20 percent of the exact response. Alavi [20] described this phenomenon for MDOF behavior under a particular type pulse signal (e.g., rectangular or harmonic). They found that the first mode behavior could represent the MDOF response when the building fundamental period is less than the pulse period. Examining a large number of near fault records, the present study confirms this conclusion, and defines an approximate T/T_p limit for a representation of local displacement demands by fundamental mode.

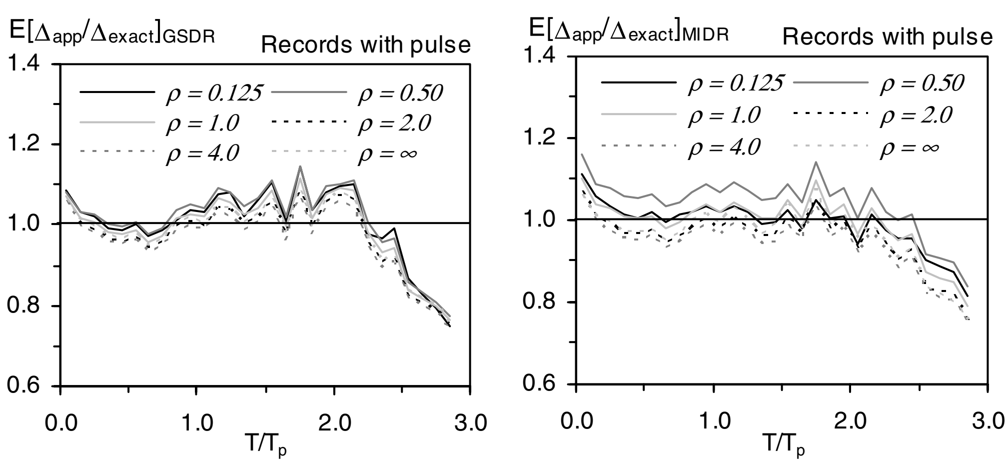

Figure 6. Mean error statistics for the near-fault records that have pulse signals

A similar evaluation for the near-fault records without a pulse signal in their velocity waveforms is presented in Figure 7. The plots show that for fundamental periods between 0.3s and 2.0s, the approximate method estimates the mean variation of MIDR and GSDR within an error limit of 15 percent to –10 percent. The estimates are better for GSDR values. Both in Figures 6 and 7 the estimates are sensitive to the variation in ρ which is more apparent in MIDR. The mean errors tend to shift towards unsafe side as ρ and T increase. The dominance of higher mode effects in the long periods is the primary cause of the unsafe predictions. The standard deviation of the approximate method for MIDR to describe the dispersion on the mean estimates is presented in Figure 8. The period and ρ-dependent standard deviation is less than 0.1 when T/T_p and T are less than 1.5 and 1.5s for the ground motions with and without pulse, respectively. The complementary standard deviation statistics and the general observations made from mean error curves suggest that the acceptable local displacement estimations based on the proposed procedure are limited to $T/T_p < 1.5$ and $T < 1.5$s for pulse and no pulse signal near-fault records, respectively.

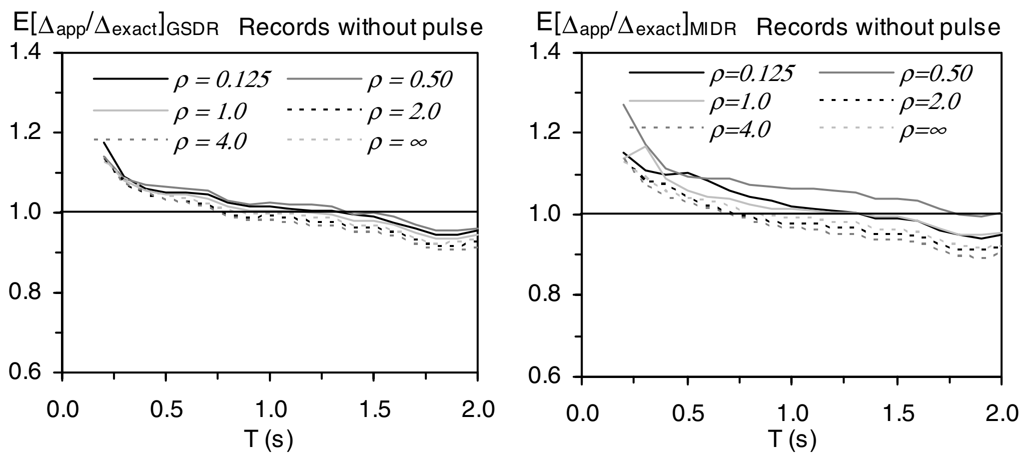

Figure 7. Mean error statistics for the near-fault records that do not exhibit pulse signals in their waveforms

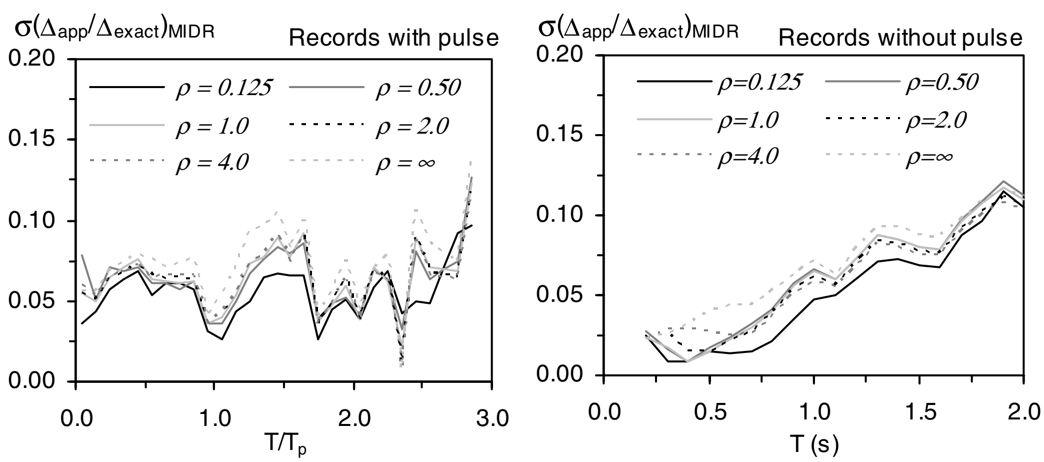

Figure 8. Dispersion of the proposed procedure

These observations point that the first mode contribution yields fairly good estimates of the exact response for a relatively wide range of structural periods that are usually the concern in many engineering applications. Caution should be exercised as the use of first mode behavior may cause significant errors for long period systems when they are subjected to near-fault records with or without pulse effects.

COMPARISONS WITH SIMILAR METHODS

A similar statistical verification is applied to the procedures proposed by Iwan [10] and Miranda [13] that can be used for estimating the maximum local displacement demands on structural systems. Iwan [10] uses the ground velocity and displacement wave trains traveling along the height of a continuous shear beam and computes the maximum shear strain due to reflection and refraction of these waves between the tip and bottom of beam. The shear strain is analogous to interstory drift. The method of Miranda [13] is more general, and describes the maximum interstory drift through a fourth order differential equation. This procedure considers the shear and flexural behavior through the variable α that has a similar effect as ρ in this study. A value of $\alpha = 0$ is pure flexural behavior and $\alpha = \infty$ represents pure shear behavior. Miranda [14] propose $\alpha = 10$ for a general MRF behavior. Miranda [13, 14] indicated that a fairly good shear frame behavior can be simulated by assigning a value greater than 30 for α. The expressions proposed by Iwan [10] and Miranda [13] are shown in Equations (16) and (17), respectively.

$$D_r(T,\xi) = \max_{\forall t} \frac{1}{c}\left| v(t) + \frac{2\pi\xi}{T} z(t) + 2 \sum_{n=1}^{N \le 2t/T} (-1)^n \exp(-n\pi\xi)\left[v(t - n\frac{T}{2}) + \frac{2\pi\xi}{T} z(t - n\frac{T}{2})\right]\right| \tag{16}$$

$$IDR_{\max}(T,\xi) = \beta_1 \beta_2 \frac{S_d(T,\xi)}{H}; \quad \beta_2 = \left| \frac{C_1 \alpha \cosh \alpha \frac{y}{H} + C_2 \alpha \sinh \alpha \frac{y}{H} + C_3 a e^{-az/H} + 2C_4 \frac{y}{H} + C_5}{C_1 \sinh \alpha + C_2 \cosh \alpha + C_3 e^{-a} + C_4 + C_5 + C_6} \right|_{\max} \tag{17}$$

In Equation (16), D_r denotes the maximum ground story drift for a given ξ and T value. The variables v, z, and c are the ground velocity, ground displacement and shear wave velocity traveling along the shear beam, respectively. A direct relationship between T and c can be established by using T=4H/c. A more general version of Equation (16) is also proposed by Iwan [10] to account for the possibility of maximum interstory drifts occurring at building heights other than at the ground level. The comparisons of the author on the general drift expression and Equation (16) show that the ground level is generally the most critical location for maximum interstory drift. This is consistent with the general shear beam behavior where the maximum shear strains are at the ground level. In Equation (17), β_1 is the modal participation factor of the continuum model fundamental mode proposed by Miranda [13]. The modifying factor β_2 is the ratio between maximum interstory and top story drift (top story displacement normalized by the building height, H). The variables C_1-C_6 depend on α and the parameter a controls the lateral load distribution along the building height. Thus, Miranda [13] modifies the top story displacement by β_2 to approximate the maximum interstory drift ratio (IDR_{max}) whereas this study computes the maximum interstory drift by modifying the ground story drift through γ_2.

The mean error comparisons of these two methods with the procedure presented in this study are shown in Figure 9. The mean error curves computed for Miranda and proposed method follow a very similar trend for shear frame behavior. Iwan's method yields very conservative estimates for T < 0.6s. For fundamental periods less than 0.6s, the average maximum ground story drift estimates obtained from Iwan [10] grow asymptotically up to 3 times the exact mean drift results. When MRF behavior is considered, the comparisons between Miranda [13] and this study show that $\alpha = 10$ describes the general behavior fairly well. The estimations of this study and Miranda [13] follow the same trend when ρ takes a value of 2. The expression in Equation (17) yields slightly unsafe maximum interstory drift approximations than the proposed method in long period structures for other ρ values considered in the comparison. The standard deviation curves for Miranda is very similar to those presented in Fig 8. The analytical expressions for *GSDR* and *MIDR* proposed by this study are relatively simple with respect to the other two procedures compared in this section.

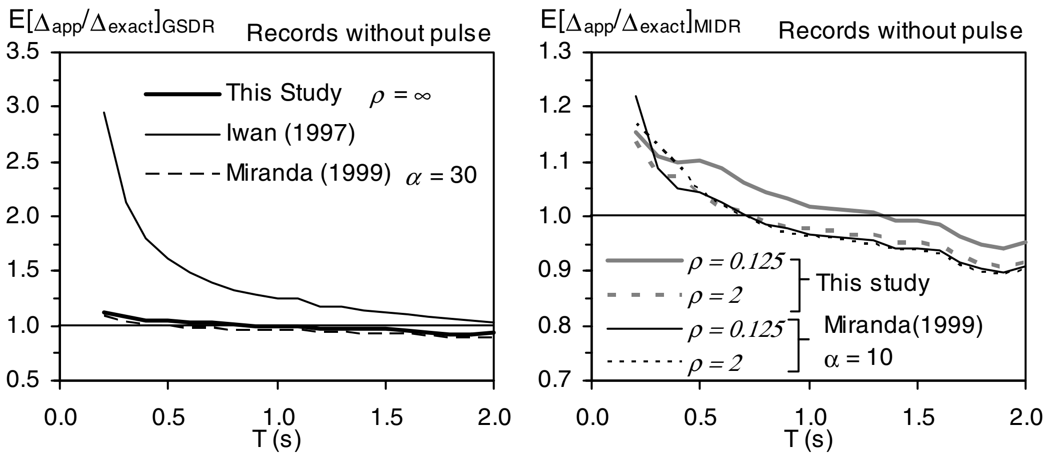

Figure 9. Comparison of mean error statistics with other procedures

SUMMARY AND CONCLUSIONS

Two simple expressions for estimating the ground story and maximum interstory drift ratios are presented. These expressions are used to modify the drift expression of Gülkan [16] by considering the beam-to-column stiffness ratio. The theoretical fundamental mode behavior of frame structures is used in the derivation of these expressions. The proposed procedure gives a direct estimation of critical local deformation demands making it useful for the preliminary design or an elementary displacement based performance assessment. A total of 145 near-fault ground motions recorded on dense-to-firm soil sites are used for the evaluation of proposed expressions. Of the near-fault ground motion data set 56 records contain pulses in their waveforms. The evaluations are done separately for ground motion records with and without pulses, and exact demands computed from response history analyses are compared statistically with the estimated values using the proposed procedure. The statistical verifications are based on the mean errors and their dispersions. The new method is also compared with Iwan [10] and Miranda [13] expressions to give complete information for similar procedures that can be used as tools in seismic design and assessment methodologies. The following observations and conclusion are made:

1. The ground story drift is sensitive to the variation in beam-to-column stiffness ratio (ρ). Estimates made by shear beam behavior (ρ = ∞) may produce very conservative results for ground story displacement of frame structures that display lateral deformations both in shear and flexure.
2. The pulse signal effect on the ground story (GSDR) and maximum interstory drift (MIDR) demands have been confirmed by using a large amount of near-fault records with pulse. These local displacement demand parameters tend to become amplified when the fundamental period (T) of the structure takes values closer to the pulse period (T_p) of the excitation.
3. Considering the first mode behavior, the proposed procedure can represent GSDR and MIDR with acceptable accuracy for near-fault records with pulse when T/T_p values are less than 1.5. The error is within ± 10 percent with respect to the mean variation of exact response for $T/T_p < 1.5$. In the case of near-fault records without pulse, the first mode can represent the actual GSDR and MIDR demand fairly well for T < 1.5s. Under the near-fault records with no pulse, the

approximations produce errors of ± 15 percent with respect to the mean of exact response for a fundamental period range of 0.3s to 1.5s.

4. The comparisons with other similar procedures show that the method of Iwan [10] tends to overestimate the local displacement demands significantly for T < 0.6s. The proposed method and Miranda [13] expression yield similar results for frame structures that undergo deformations both in flexure and shear.

ACKNOWLEDGEMENTS

The "Research Projects Grant" of the Middle East Technical University funded the second author during the conduct of this study.

REFERENCES

1. Earthquake Engineering Research Institute (EERI). "Northridge earthquake of January 17, 1994 reconnaissance report," Hall J, Editor, Earthquake Spectra 1995; Supplementary C to Vol. 11.
2. Sasani M, Bertero VV. "Importance of severe pulse-type ground motions in performance-based engineering: historical and critical review." Proceedings of the 12th World Conference on Earthquake Engineering, Auckland, New Zealand, Paper No. 1302, 2000.
3. Gupta A, Krawinkler H. "Behavior of ductile SMRFs at various seismic hazard levels." Journal of Structural Engineering, ASCE 2000; 126(1): 98-107.
4. Luco N, Cornell CA. "Effects of connection fractures on SMRF seismic drift demands." Journal of Structural Engineering, ASCE 2000; 126(1): 127-136.
5. MacRae GA, Mattheis J. "Three-dimensional steel building response to near-fault motions." Journal of Structural Engineering, ASCE 2000; 126(1): 117-126.
6. Attalla RM, Paret TF, Freeman SA. "Near-source behavior of buildings under pulse type earthquakes." Proceedings of the 6th U.S. National Conference on Earthquake Engineering, Seattle, Washington, Paper No. 270. 1998.
7. Krawinkler H, Medina R, Alavi B. "Seismic drift and ductility demands and their dependence on ground motions." Engineering Structures 2003; 25(5): 637-653.
8. Westergaard HM. "Earthquake-shock transmission in tall buildings." Engineering News-Record, 1993, November.
9. Heidebrecht AC, Stafford Smith B. ''Approximate analysis of tall wall-frame structures.'' Journal of the Structural Division, ASCE 1973; 99(2): 199–221.
10. Iwan WD. "The drift spectrum: a measure of demand for earthquake ground motions." Journal of Structural Engineering, ASCE 1997; 123(4): 397-404.
11. Heidebrecht AC, Naumoski ND. "Development and application of a displacement-based design approach for moment-resisting frame structures." Fajfar P, Krawinkler H, Editors. Seismic design methodologies for the next generation of codes, Roterdam: AA Balkema, 1997: 217-228.
12. Heidebrecht, AC, Rutenberg A. "Applications of drift spectra in seismic design." Proceedings of the 12th World Conference on Earthquake Engineering, Auckland, New Zealand, Paper No. 209, 2000.
13. Miranda E. "Approximate seismic lateral deformation demands in multistory buildings." Journal of Structural Engineering, ASCE 1999; 125(4): 117-126.
14. Miranda E, Reyes CJ. "Approximate lateral deformation demands in multistory buildings with nonuniform stiffness." Journal of Structural Engineering, ASCE 2002; 128(7): 117-126.

15. Chopra AK, Chintanapakdee C. “Drift spectrum vs. modal analysis of structural response to near-fault ground motions.” Earthquake Spectra 2001; 17(2): 221-234.
16. Gülkan P, Akkar S. “A simple replacement for the drift spectrum.” Engineering Structures 2002; 24(11): 1477-1484.
17. Blume JA. “Dynamic characteristics of multi-story buildings.” Journal of the Structural Division, ASCE 1968; 94(2): 377-402.
18. Seneviretna GDPK, Krawinkler H. “Evaluation of inelastic mdof effects for seismic design.” Report No. 120, The John A. Blume Earthquake Engineering Center, Stanford University, Stanford, CA, 1997.
19. Akkar S, Yazgan U, Gülkan P. “Deformation limits for simple non-degrading systems subjected to near-fault ground motions.” Proceedings of the 13th World Conference on Earthquake Engineering, Vancouver, B.C., Canada, Paper No. 2276, 2004.
20. Alavi B, Krawinkler H. “Effects of near-fault ground motion on frame structures.” Report No. 138, The John A. Blume Earthquake Engineering Center, Stanford University, Stanford, CA, 2001.